International Journal of Impact Engineering 195 (2025) 105146

Contents lists available at ScienceDirect

International Journal of Impact Engineering

journal homepage: www.elsevier.com/locate/ijimpeng

Performance assessment of an innovative light and compact dust shield for DISC onboard Comet Interceptor/ESA space probes

Vincenzo Della Corte [a,*], Stefano Ferretti [b,c], Alice Maria Piccirillo [a], Alessandra Rotundi [b,c], Ivano Bertini [b,c], Fabio Cozzolino [a], Alessio Ferone [b], Stefano Fiscale [b], Andrea Longobardo [c], Laura Inno [b], Eleonora Ammannito [d], Giuseppe Sindoni [d], Chiara Grappasonni [d], Matthew Sylvest [e], Manish R. Patel [e], Hanno Ertel [f], Mark Millinger [f], Hanna Rothkaehl [g]

[a] Osservatorio Astronomico di Capodimonte, Istituto Nazionale di Astrofisica, Salita Moiariello, 16, 80131, Naples, Italy
[b] Dipartimento di Scienze e Tecnologie, Università degli Studi di Napoli "Parthenope", CDN, IC4, 80143, Naples, Italy
[c] Istituto di Astrofisica e Planetologia Spaziali, Istituto Nazionale di Astrofisica, Via del Fosso del Cavaliere, 100, 00133, Rome, Italy
[d] Italian Space Agency (ASI), Via del Politecnico snc, 00133, Rome, Italy
[e] School of Physical Sciences, The Open University, Walton Hall, Kents Hill, MK7 6AA, Milton Keynes, UK
[f] ESTEC–European Space Research and Technology Centre, Keplerlaan 1, Noordwijk aan Zee, Netherlands
[g] Space Research Centre, Polish Academy of Sciences, 00-716, Warsaw, Poland

ARTICLE INFO

Keywords:
Hypervelocity impacts
Cometary dust
Whipple shield
Aerogel
Ballistic limit equation

ABSTRACT

The dust ejected by cometary nuclei encodes valuable information on the formation and evolution of the early Solar System. Multiple short-period comets have been studied in situ, but several perihelion passages considerably modified their pristine condition. Comet Interceptor is the first space mission selected by the European Space Agency to study a pristine dynamically new comet in situ. During a fast flyby through the comet coma, hypervelocity impacts with dust particles will represent not only an important source of information, but also a serious hazard to the spacecraft and its payload. Here we discuss the assessment tests performed on the dust shield of the Dust Impact Sensor and Counter instrument (DISC), part of the Comet Interceptor payload, which will be directly exposed to the cometary dust flux. Using a Light-Gas Gun, we shot mm-sized particles at ~5 km/s, transferring momenta and kinetic energies representative of those foreseen for the mission. The impact effects on the DISC breadboard were compared to theoretical predictions by a ballistic limit equation for hypervelocity impacts. We find that, with a simple improvement in the dust shield design, DISC is compatible with the expected cometary environment.

1. Introduction

In the last three centuries, many scientists from different disciplines devoted great efforts to discover the origin of the Solar System [1,2]. As well preserved remnants of most ancient bodies, comets provide a direct memory of how pebbles and planetesimals turned into planets in the protoplanetary disk [3]. In particular, essential details on the formation and evolution of the early Solar System are encoded in the dust ejected by cometary nuclei.

Multiple short-period comets (SPCs) have already been studied in situ [4] with great scientific return, e.g. from Giotto [5] and Rosetta [6] space missions. The former, supported by the VEGA spacecrafts (S/Cs) [7], captured high-resolution images of comet 1P/Halley and studied its nucleus [8,9]. The latter monitored the activity of comet 67P/Churyumov-Gerasimenko nucleus before and after perihelion, providing important insight into the comet composition [10], surface [11–14], and inner coma dynamics [15–20]. Due to multiple passages at the perihelion, SPCs are highly-evolved objects showing radical changes from their formation in the outer layers. So, questions arose on which properties are primordial and which come from evolutionary processes. To solve this puzzle, further pristine comets need to be studied while first inbound in the inner Solar System.

Comet Interceptor (CI), which includes three different S/Cs, is the first F-class space mission selected by the European Space Agency (ESA) to study in situ a dynamically new comet (DNC), e.g. a long-period comet from the Oort cloud entering the inner Solar System for the first time [21], or an interstellar object originating at another star [22]. DNCs are usually discovered no more than a few years before

* Corresponding author.
E-mail address: vincenzo.dellacorte@inaf.it (V. Della Corte).

https://doi.org/10.1016/j.ijimpeng.2024.105146
Received 11 February 2024; Received in revised form 23 September 2024; Accepted 14 October 2024
Available online 24 October 2024

perihelion, too late considering the lead-up time to plan and launch a space mission. CI's innovative and flexible approach allows the mission to be developed before target identification. The S/C will orbit the Sun-Earth L2 Lagrange point for up to 3 years. After target identification, CI will follow a detailed intercept trajectory to perform multi-point measurements of the comet during a fast flyby (between 10 km/s and 70 km/s) through the coma. The mother S/C A, kept at a relatively high distance from the nucleus (~1000 km), will deploy two smaller probes (B1 and B2) that will flyby at closer distances to perform high-risk but high-return measurements.

Our team, after the development of the GIADA Impact Sensor, successfully flown onboard the Rosetta space probe [23,24], is now in charge of developing the Dust Impact Sensor and Counter (DISC), one of the instruments included in the Dust Field and Plasma (DFP) suite [25], part of the CI payload. Provided in two units, mounted on S/Cs A and B2, DISC will: study cometary dust particles with diameter of 1–400 μm; determine the dust mass distribution in the range $10^{-15}-10^{-8}$ kg; count the number of particles with mass $m > 10^{-15}$ kg; retrieve information on particle density/structure [26,27]. Given the S/C flyby speed as the particle's speed, these results can be obtained from the momentum of particles impinging on the DISC sensing surface. DISC impact plate will be directly exposed to the cometary dust environment, so hypervelocity impacts (HVIs) will represent a major risk during the CI close flyby and a proper dust shield to protect internal parts of DISC is necessary.

Modern dust shields are usually derived from the Whipple shield [28], a simple dual-sheet structure composed of a thin front bumper and a rear wall with some space in between. The front sheet breaks up on impact and divides the colliding particle in many fragments that fan out, so that the energy at the rear wall is distributed over a larger area. This design has been widely employed in last decades space missions, with dedicated upgrades according to specific conditions. The CONTOUR/NASA S/C, for instance, was planned to fly through the coma of comets Encke and Schwassmann-Wachmann-67 at speeds of 28.2 km/s and 14 km/s, respectively [29], however the spacecraft was lost when attempting to leave the earth orbit. It was protected by a multishock dust shield made of four equally spaced Nextel bumpers spaced 63.5 mm from the rear kevlar wall, for a total standoff distance of 254 mm. A similar solution was adopted for Stardust/NASA space mission, which explored the coma of comet 81P/Wild 2 at 6.12 km/s [30]. In this case, the dust shield consisted in a front composite panel bumper followed by three equally spaced layers of Nextel ceramic cloth, and a composite panel as the catcher shield in the back which also formed the structural end of the S/C bus. Closer conditions to those foreseen for CI were faced by Giotto S/C, which flew 596 km (at close approach) far from the Halley's comet nucleus at 68 km/s [31]. Its dust shield was made of a 1 mm-thick aluminum front sheet, spaced 23 cm from the 7 cm-thick rear sheet composed of various layers of epoxy kevlar, polyurethane foam, ML1 (Mylar), and aluminum honeycomb. Due to mass and volume budgets, however, we developed a lighter and more compact solution for DISC dust shield. In particular, we integrated the basic Whipple shield with an aerogel layer between the front bumper and the rear wall, in order to improve its mechanical resistance.

In this paper we report on the test campaign carried out on the DISC dust shield to verify its compatibility with the expected cometary conditions. We submitted the unit to HVIs with mm-sized projectiles releasing momenta of $10^{-2}-10^{-1}$ kg m/s and energies of the order of 10^2 J. Theoretical predictions by a ballistic limit equation for HVIs allowed a proper analysis of the DISC dust shield response. A simple improvement to the dust shield design lowers DISC risk of failure below the threshold value of 10%. The upgraded design ensures high-level mechanical protection and is then compatible with the expected cometary environment.

2. Materials and methods

DISC consists in a 121 × 115.5 × 68 mm^3 parallelepiped-shaped aluminum box, which contains the acquisition system and the dust shield against hazardous impacts. A detailed DISC design is reported in Fig. 1, panel (a). DISC detection system consists of a 100 × 100 mm^2 square aluminum plate (i.e. the sensing plate), 0.5 mm in thickness, and three NCE51 NOLIAC(tm) ceramic equivalent piezoelectric transducers (PZTs) glued at its corners. A further PZT, glued at the fourth corner of the plate, acts as internal calibrator during in-orbit operations. When a dust particle collides on the aluminum plate, acoustic Lamb waves [32] form and propagate up to the PZTs that start to vibrate at their resonant frequency (200 kHz) responding to mechanical solicitations with an induced voltage, which encodes information on the impacting particle momentum. The signal is collected and processed by the electronics housed at the bottom of the aluminum box; the electronics are shielded by four 12 mm-thick aerogel blocks embedded in a 1.5 mm-thick aluminum frame (i.e. the dust shield frame). A baffle on the edges of the aluminum plate defines the DISC sensing area (84 × 84 mm^2) ensuring a threshold minimum distance between any impact point and the closest PZT. Indeed, as reported by Liu et al. [33], shock waves resulting from HVIs evolve in mechanical waves at short distance (~8 mm) from the impact.

During the CI scientific phase, DISC will be directly exposed to the flux of dust particles ejected from the target comet nucleus to measure their momenta and energies, respectively in the ranges $10^{-11}-10^{-3}$ kg m/s and $10^{-7}-10^{2}$ J [34]. While GIADA Impact Sensor onboard Rosetta was designed for a low-speed (<100 m/s) dust particles environment, the fast CI flyby (10–70 km/s) will expose DISC to much more challenging conditions in terms of dust hazards. In particular, DISC onboard S/C B2 will face the most hazardous scenario since it will fly closer to the comet nucleus (~300 km) than S/C A (~1000 km). With a probability around 20%, S/C B2 will collide with mm-sized dust particles at a speed possibly up to 70 km/s [35]. Such HVIs are likely to damage the DISC sensing plate, but with very minor effects on its measurement capability. Conversely, the electronics might be seriously threatened and need to be properly protected from the dusty environment. To this aim we developed a dedicated and unconventional dust shield, to be integrated under the DISC sensing plate and above the electronics, and tested its performance by shooting mm-sized particles with the Light-Gas Gun (LGG) operating at The Open University, in Milton Keynes, UK [36,37].

2.1. DISC dust shield design

Developing an optimized DISC dust shield, within the resources (mass and volume) available in the CI space mission frame, could not follow the adoption of a standard solution such as the Whipple shield [28], which is not expected to stop an impacting particle nor to significantly dissipate its energy. It fragments the particle, whose energy is dispersed among the many debris that fan out between the bumper and the S/C wall. For the dust impacts foreseen in the frame of CI, this solution, even a pile of several layers, would require dimensions along the impact direction and masses that are prohibitive for the resources assigned to DISC. We overcame these limitations by developing a never-used-before customized configuration of the dust shield to meet DISC needs coupled with CI requirements. As shown in Fig. 2, panel (a), the DISC sensing plate, besides transmitting impact waves to the DISC sensors (i.e. the PZTs), also acts as the first bumper of the conventional Whipple shield, i.e. it breaks up the hyper speed dust particles on impact. To slow down and finally stop the resulting cloud of debris, we inserted a 12 mm-thick aerogel layer just below the sensing plate (along the path of incoming particles). The structural element housing the aerogel is a light aluminum frame of 1.5 mm thickness. In the current design, the DISC dust shield is a very compact element (Fig. 2, panel (b)) of a total mass of 58 g (53 g the mechanics, 5 g

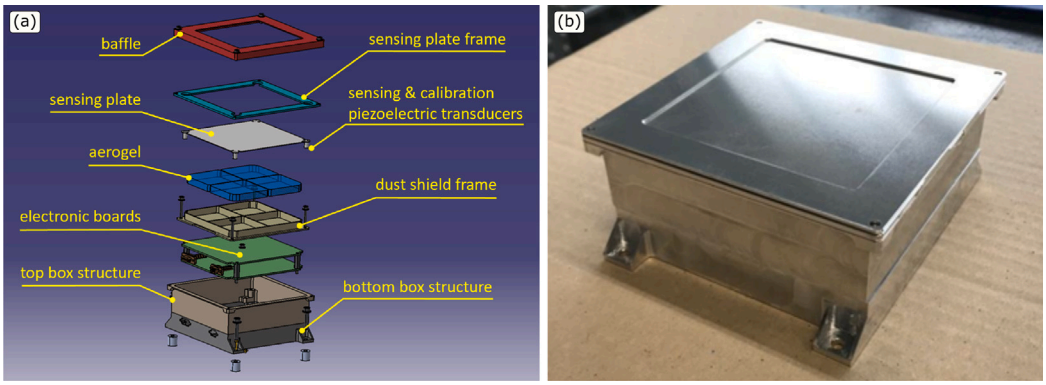

Fig. 1. (a) Exploded view showing the Dust Impact Sensor and Counter (DISC) instrument components. When a cometary dust particle impacts the upper 0.5 mm-thick aluminum sensing plate, mechanical vibrations propagate up to its corners. Following such vibrations profile, three piezoelectric transducers (a fourth one acts as internal calibrator) generate an electrical signal, which is then processed for data extraction. A dedicated 1.5 mm-thick aluminum frame, embedding four thick aerogel blocks, shields the electronics from hazardous impacts. Panel (b) shows the assembled DISC breadboard.

Fig. 2. (a) Scheme and (b) picture of our innovative light and compact dust shield for DISC breadboard inspired by the Whipple dust shielding principle: in the event of a collision with a hyper speed projectile, a thin bumper (the DISC sensing plate) breaks up the impacting particle into a cloud of debris that fan out. In order to slow down and stop hypervelocity particle fragments, we added a thick aerogel layer (10 mm in the configuration used for tests) between the DISC sensing plate and the bottom of the dust shield (dust shield frame). When the fragments reach the dust shield frame, their energy has been properly dispersed, thus the impact hazard level for the electronics is significantly reduced.

the aerogel). A potential increase in the aerogel block thickness would result in a negligible impact on the instrument mass.

Successful application of aerogel in space, laboratory tests and models inspired us to select this material as a suitable solution for a compact and light design for DISC dust shield. In addition to its exceptional ability to decelerate and capture fast moving dust particles, aerogel also has unusual properties, e.g. low values of thermal conductivity, refractive index and sound speed propagation. Several samples of aerogel blocks directly exposed to dust flux in space in low Earth orbit were able to capture particles at speeds up to tens of km/s. Aerogel was used on the space shuttle, e.g. STS flights 41-B, 41-D, 61-B [38] and on STS 42, 47, 57, 60, 61, 68, 69, 72, 101 [39] and on the EuReCa satellite launched and retrieved in 1993 [40,41]. A number of experiments have exposed aerogel outside the Mir Russian space station, these include EuroMir 95 [42] and the NASA ODC experiment [43–45]. More recently, Stardust/NASA space probe, launched in 1999, captured cometary particles using aerogel during the flyby at 6 km/s in the coma of comet Wild 2 and returned them to Earth in 2006 [30]. All the above listed experiments, aimed at capturing interplanetary, cometary, and interstellar dust at hyper speed (up to tens of km/s), successfully demonstrated the aerogel capability to slow down and stop hypervelocity dust particles. Rather than carving a crater and vaporizing, a particle hitting an aerogel block tunnels in and it is caught leaving a carrot-shaped track (compact impacting particles) or a bulb track (porous impacting particles) [46–49].

The effectiveness of porous materials in slowing down and stopping solid bodies impacting at speeds higher than 4 km/s was studied by Trucano and Grady [50]. By combining numerical analyses and laboratory tests, they concluded that in the collision of a solid projectile on a porous target the penetration depth of the projectile decreases as the impact speed increases. Aerogel is an extremely porous material, characterized by nm-sized features linked in a highly porous dendritic-like structure. In order to define the aerogel ability to stop dust particles with speeds in the range expected during the CI close encounter, we refer to the work performed by Burchell et al. [49], where aerogel track lengths are analyzed as a function of the impacting speed. They performed a test campaign firing glass spheres, at speeds ranging from 1 km/s up to 7.5 km/s, in aerogel targets of different densities, demonstrating that: (1) as the projectile speed increases the track length increases reaching a maximum value after which it drops; (2) the speed value corresponding to the maximum track length increases as the aerogel density decreases. Similar tests with Al_2O_3 particles were carried out by Kitazawa et al. [51], who obtained a model that predicts the penetration track length and the diameter of impacting projectiles. In the work performed by Domínguez et al. [52], a model of impact cratering in aerogels was developed and tested. The correspondence between experiment and theory is good and indicates that the physics of impact crater formation in aerogel is well described by a model in which an outgoing cylindrical shock wave attenuates and stops when it is no longer able to overcome the mechanical strength of the aerogel. A relation between aerogel properties (mainly density) and the track length L_t left by hypervelocity particles in this medium can be expressed as:

$$L_t = \lambda \cdot \log\left(v_i/v_f\right)^2 \tag{1}$$

where v_i and v_f are the initial and final velocities of the particle and λ is given by

$$\lambda = \frac{2d}{3C}\left(\frac{\rho_i}{\rho_0}\right) \tag{2}$$

where d is the particle diameter and ρ_i is its density, ρ_0 is the density of uncompressed aerogel, and C is a parameter generally expected as ≈1. Using this equation and the parameters of the aerogel part of the DISC dust shield (Table 1), we obtained the terminal speed of particles of different diameters and density $\rho_i = 1\,\mathrm{g/cm^3}$ crossing an aerogel layer of two different thicknesses at the upper and lower limit speed foreseen for the CI flyby. These values, reported in Fig. 3, show that a 1.5 cm-thick aerogel layer can slow down also particle fragments of 200 μm in diameter impacting at the maximum speed foreseen for CI flyby (70 km/s) to speeds lower than 300 m/s.

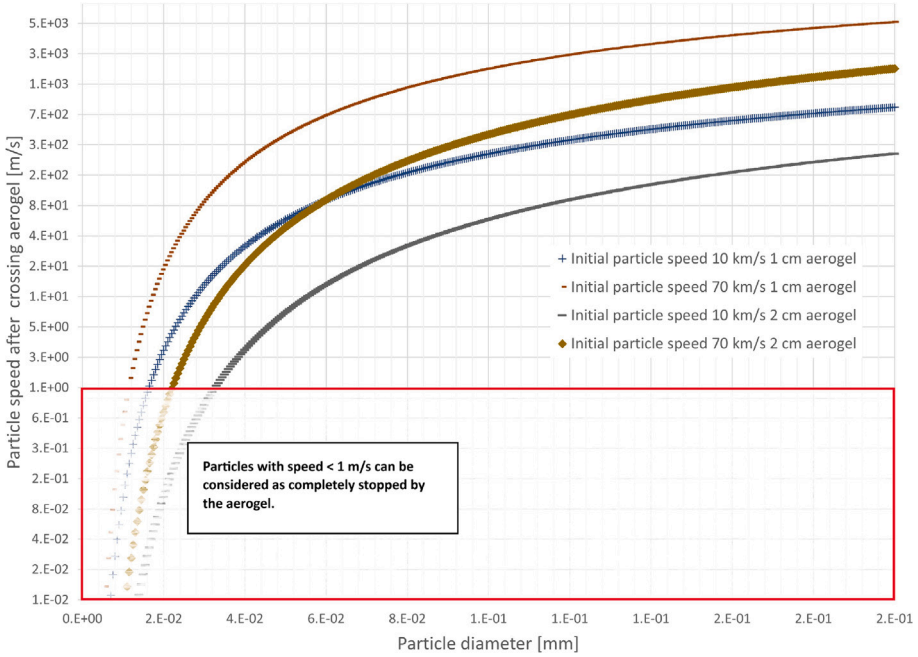

Fig. 3. Speed values of particles with size in the range 1–200 μm (density ρ_i = 570, kg/m^3 [53]) after aerogel layer (thickness of 1 cm and 2 cm) crossing and initial speeds of 10 km/s and 70 km/s, i.e. the speed limits of the Comet Interceptor flyby.

Table 1
Physical properties of the aerogel integrated into DISC dust shield (data obtained from the manufacturer *OcellusInc.*).

Property	Value
Density	0.1 (0.05–0.3) g/cm^3
Dielectric constant	1.02–1.48 (@20 GHz)
Surface area, BET	800 m^2/g
Percent solids	0.5%–14%
Mean pore diameter	~20 nm
Primary particle diameter	2–5 nm
Refractive index	1.002–1.063
Thermal tolerance	to 500 °C
Poisson's ratio	0.24
Young's modulus	0.01–10 MPa
Tensile strength	16 kPa
Fracture toughness	~0.8 kPa m$^{1/2}$
Compressive modulus	0.3 MPa
Coefficient of Thermal Expansion	2 ppm/°C @(20–80) °C
Electrical resistivity	10^{15} ohm-cm
Thermal conductivity in air	0.016 W/m/° K
Thermal conductivity in vacuum	0.004 W/m/°K
Sound velocity through the medium	<200 m/s
Transparency	>90% (visible wavelengths)

Table 2
Material and density ρ_i of LGG projectiles.
Source: https://www.matweb.com and https://www.webmineral.com/ .

Material	ρ_i (kg/m^3)
Nylon	1110
Aluminum	2700
Borosilicate glass	3000
Forsterite	3270
Stainless steel	7800

2.2. DISC dust shield assessment strategy

Space payload on-ground performance testing is fundamental for mission preparation, even though reproducing in situ measurement conditions is not always possible. DISC onboard Comet Interceptor/ESA space mission will operate in a cometary dust environment undergoing to hyper speed dust impacts (7 km/s–70 km/s), only marginally reproducible with on-ground facilities, i.e. ≤10 km/s. In order to assess the DISC dust shield performance in the CI target environment, by means of the Engineering Dust Coma Model (EDCM) [35,53], we retrieved the maximum diameter of dust particles foreseen to impact on the DISC sensing plate (84 × 84 mm^2) with a probability higher than ~10% during the flyby, being 10% the threshold probability set for the S/Cs safety.

EDCM solutions predict that most of the impacts will involve μm-sized particles, as the impact probability rapidly drops for mm-sized particles (Fig. 4). We determined a diameter of 1 mm for the largest particles impacting DISC with a probability of $P \approx 0.1$ (Fig. 4, right panel). In the most harmful situation of 70 km/s flyby speed, considering a cometary dust density of 570 kg/m^3 [53], a 1 mm impacting particle would transfer a momentum $p \sim 0.02$ kg m/s and a kinetic energy $K \sim 700$ J. In order to test if DISC can survive these conditions, we performed hypervelocity impacts by means of a two stage Light Gas Gun (LGG) firing up to mm-sized projectiles (from 250 μm to 3 mm) at speeds from 4.4 km/s to 6 km/s. Since the highest speed obtainable with this facility is lower than the lowest speed limit foreseen for CI flyby, we used larger and denser projectiles with respect to cometary dust to produce impacts with comparable kinetic energies: the assessment of impact damages on different materials can be quantified by the kinetic energy involved in the impact. When a projectile impacts an aluminum surface, the kinetic energy, which is a function of projectile mass and velocity, is transferred to the target, causing deformation and potential failure. The damage on the dust shield is linked to the ratio between the target thickness and the projectile size [54,55], i.e. the higher is the projectile diameter the worst is the shield performance. Thus, increasing the projectile size and mass to reach the expected levels of kinetic energy would imply an under evaluation of the dust shield performances

We shot particles made of the materials listed in Table 2 on the DISC breadboard at speeds around 5 km/s, which transferred momenta in the range 10^{-2}–10^{-1} kg m/s and energies of the order of 10^2 J.

3. Results and discussion

We assembled four DISC breadboards for the tests, each one was exploited for multiple shots in different areas of the sensing plate. To

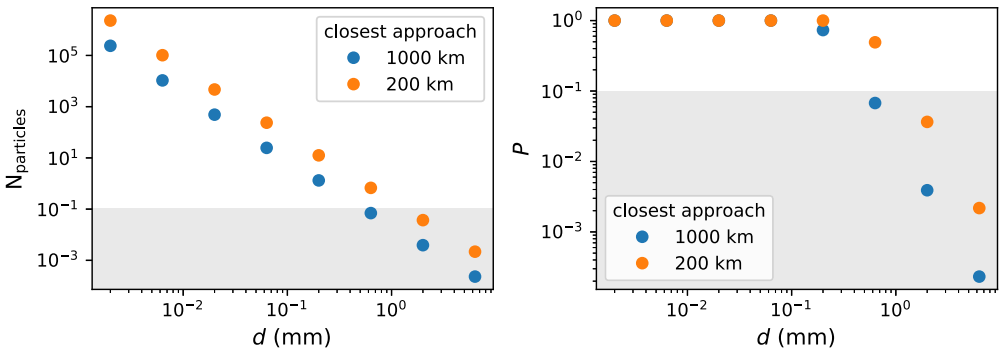

Fig. 4. Left panel: Engineering Dust Coma Model [35,53] estimate of the total number of particles $N_{particles}$ (*vs.* diameter d) hitting the DISC sensing surface during the entire flyby. Right panel: impact probability $P = 1 - \exp\left[-N_{particles}\right]$ with a particle of a given diameter. For the Engineering Dust Coma Model we considered the average activity level, i.e. of a typical target for Comet Interceptor, and at the two closest approach distances for S/C A (cyan) and S/C B2 (orange). The greyish area highlights the region where $P < 0.1$, being 0.1 the threshold probability set for the S/Cs safety.

classify the tests results we define a dust shield "failure" when the impacting particle perforates the "dust shield frame" (see Fig. 1). In fact, this implies that the electronics has not been protected by the dust shield.

In Fig. 5 we report the effects of three shots performed on the DISC breadboard #1 using the following projectiles: a first shot using a 1 mm stainless steel sphere and two additional shots using a 3 mm nylon sphere (further data in Table 3). The 1 mm stainless steel bead passed through the aluminum sensing plate, then the aerogel slowed down the particle and allowed the dust shield frame to definitely stop it (Fig. 5, panels (a)–(c)). The DISC dust shield frame is only affected by a small deformation and we found some metallic deposits on it, with no signs of spallation nor perforation. The confined damaged region in the aerogel suggests that the particle fragmentation was very limited or even absent, which is not a typical behavior expected for cometary dust impacts. On the contrary, the nylon beads showed a response similar to what we expect for cometary dust, whose density is comparable to nylon's. During the first attempt with the nylon bead projectile, it arrived on the DISC sensing plate completely fragmented: the projectile unfortunately impacted on the final component of the LGG and shattered. As shown in Fig. 5, panels (d)–(e), the cloud of fragments perforated the sensing plate close to the hole procured by the previous shot with the stainless steel bead and the already cracked aerogel block stopped the projectile fragments with no evident problems. Due to the projectile pre-fragmentation, however, the shot precise parameters are undefined. The test with the second nylon bead was successful (Fig. 5, panels (f)–(h)). The particle crossed the DISC sensing plate in an undamaged region. The cloud of pits in the dust shield frame (Fig. 5, panel (h)) proves that the bead fragmented on impact and the fragments were slowed down by the aerogel (already cracked because of previous shots and extremely damaged after this third shot) and finally stopped. The dust shield correctly protected DISC.

Fig. 6 shows the effects of three tests performed on the DISC breadboard #2 using the following projectiles: a first shot using a buckshot of forsterite particles with diameters ranging from 250 μm to 500 μm, and two additional shots using two aluminum beads of 2 mm and 3 mm diameter, respectively (further details in Table 4). Among the materials we used, forsterite more closely simulates the collision dynamics of cometary dust particles. The damage caused by this shot on the DISC sensing plate is very limited and the forsterite fragments were easily stopped by the first millimeters of the aerogel (Fig. 6, panels (a)–(c)). Conversely, the aluminum spheres caused heavy damage to the dust shield and beyond. Fig. 6, panel (e) shows the aerogel status after the 2 mm sphere impact at 5 km/s. The dark regions in the aerogel are due to some metallic matter that melted on impact and then spread throughout behind the sensing plate, as can be deduced from Fig. 6, panel (f). After slowdown in the aerogel, the sphere was stopped by

Table 3
Shots on DISC breadboard #1: particles of different material, diameter d and initial speed v_i transferred momentum p and kinetic energy K.

Shot #	Material	d (mm)	v_i (km/s)	p (kg m/s)	K (J)
1	Stainless steel	1	4.5	0.018	41.4
2	Nylon (fragments)	3	6.0		
3	Nylon	3	5.5	0.086	237.3

Table 4
Shots on DISC breadboard #2: particles of different material, diameter d and initial speed v_i transferred momentum p and kinetic energy K.

Shot #	Material	d (mm)	v_i (km/s)	p (kg m/s)	K (J)
4	Forsterite (buckshot)	0.25–0.50	~5.0		
5	Aluminum	2	5.0	0.057	141.4
6	Aluminum	3	5.0	0.191	477.1

Table 5
Shots on DISC breadboards #3 and #4: particles of different material, diameter d and initial speed v_i transferred momentum p and kinetic energy K.

Shot #	Material	d (mm)	v_i (km/s)	p (kg m/s)	K (J)
7	Aluminum	2	5.0	0.057	141.4
8	Aluminum	3	5.0	0.191	477.1
9	Borosilicate glass	3	4.4	0.184	404.6

the dust shield frame, where it made a bump with a small hole in the center. The most destructive effects were induced by the impact of a 3 mm aluminum sphere at 5 km/s. Despite part of the energy was absorbed by the aerogel, which completely fragmented (Fig. 6, panel (h)), the bead made a holed crater on the dust shield frame (Fig. 6, panel (i)). Part of the molten material and aerogel fragments passed through the hole and spread beyond the electronic components down to the bottom box structure of DISC (Fig. 6, panel (j)). The reason for such a damage lies in the collision dynamics: on impact, the aluminum bead probably broke up in big fragments that directly hit the dust shield frame instead of the aerogel, which did not slow down the fragments; destructive consequences resulted on the dust shield as well. The impact conditions experienced in this specific test are actually quite unlikely: they are mainly due to the dust shield frame design combined with the DISC breadboard accommodation in the LGG chamber. Indeed, the alignment of the LGG forces shooting the particles at the target center; for DISC this corresponds to the center of the dust shield frame, i.e. at the intersection of the aluminum bars dividing the four aerogel blocks. To overcome this issue, we designed and manufactured a new customized dust shield frame housing a single aerogel block (Fig. 7, panel (c)). This new frame was integrated into DISC breadboards #3 and #4 for the successive tests.

The parameters used for the third test session are reported in Table 5, the images of the tests results are displayed in Fig. 7. The

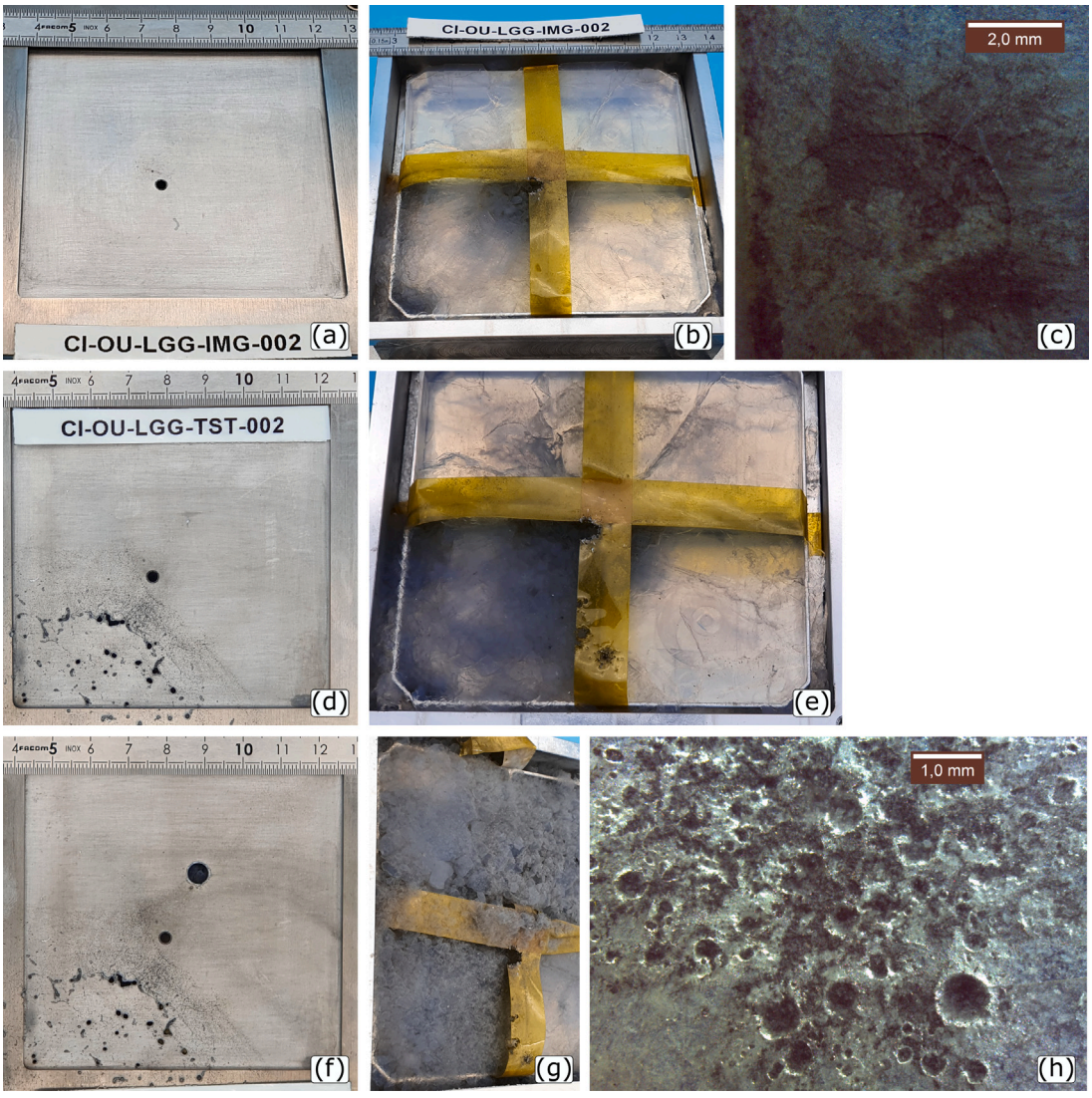

Fig. 5. DISC breadboard #1 after the impact of (in order): a 1 mm stainless steel sphere at 4.5 km/s (sensing plate (a), aerogel blocks (b), dust shield frame (c)); fragments of a 3 mm nylon sphere at 6 km/s (sensing plate (d), aerogel (e)); a 3 mm nylon sphere at 5.5 km/s (sensing plate (f), aerogel (g), dust shield frame (h)).

tests with the aluminum spheres fired on breadboard #2 were repeated on breadboard #3 using two aluminum projectiles identical to the previous ones. The result of the successful shot with the 2 mm sphere is shown in Fig. 7, panels (a)–(b): the particle hit the center of the aerogel block, which correctly slowed down the fragments; the dust shield frame presents only some deposits of molten material, but no mechanical deformations nor holes. The 3 mm sphere shot was not clean: along its path inside the LGG, the projectile gathered some debris of comparable size, left-over of previous shots, and all such particles hit the breadboard contemporary (Fig. 7, panel (d)). They produced heavy damage both on the aerogel (Fig. 7, panel (e)) and on the dust shield frame (Fig. 7, panel (f)). We cannot consider this test valid since the combined effect of simultaneous collisions from multiple projectiles is not informative. A further test was performed by firing a 3 mm borosilicate glass sphere at 4.4 km/s on breadboard #4 (Fig. 7, panels (g)–(i)). The shot was successful, the projectile hit the central region of the DISC sensing plate and completely perforated the dust shield. We consider the result of this test to fix the minimum energy impact implying a dust shield failure.

For a meaningful analysis of the DISC dust shield performance we focused on the projectile kinetic energy, that is the dominant parameter governing crater formation from HVIs [56,57]. For a preliminary qualitative rescaling of our results to the foreseen cometary environment, we computed the "corresponding diameter" d_K^* for which a (spherical) cometary dust particle with a density of 570 kg/m^3 impacting at 70 km/s would have the kinetic energy released by the described LGG tests. Table 6 and Fig. 8 report the corresponding diameters for the experiments we performed, together with the EDCM estimated impact probability (P_K^{B2}) on DISC onboard S/C B2 (flyby closest approach: 200 km), which is the reference for our tests evaluation as it represents the worst case. The table also reports the impact probability (P_K^A) on DISC onboard S/C A (flyby closest approach: 1000 km). According to this computation, for DISC onboard S/C A the probability of an impacting particle classified as a "failure projectile" (highlighted in gray in Fig. 8) is below the threshold value of 10% ($P_K^A \sim 3\%$–4%), thus compliant with the S/C safety requirements. Conversely, cometary dust particles with kinetic energy comparable to the "failure projectiles" energy are too likely to impact on DISC onboard S/C B2 ($P_K^{B2} \sim 30\%$) with respect to the S/C safety requirements.

This strategy does not consider the different collision dynamics among particles with different physical properties, which actually plays a fundamental role. The proper functioning of a dust shield derived from the Whipple shield, as for DISC, relies on particle fragmentation at impact. However, not all the projectiles we used for the tests undergo this physical process under the conditions of our experiments. In order to compare our results to a more reliable reference, we used a more

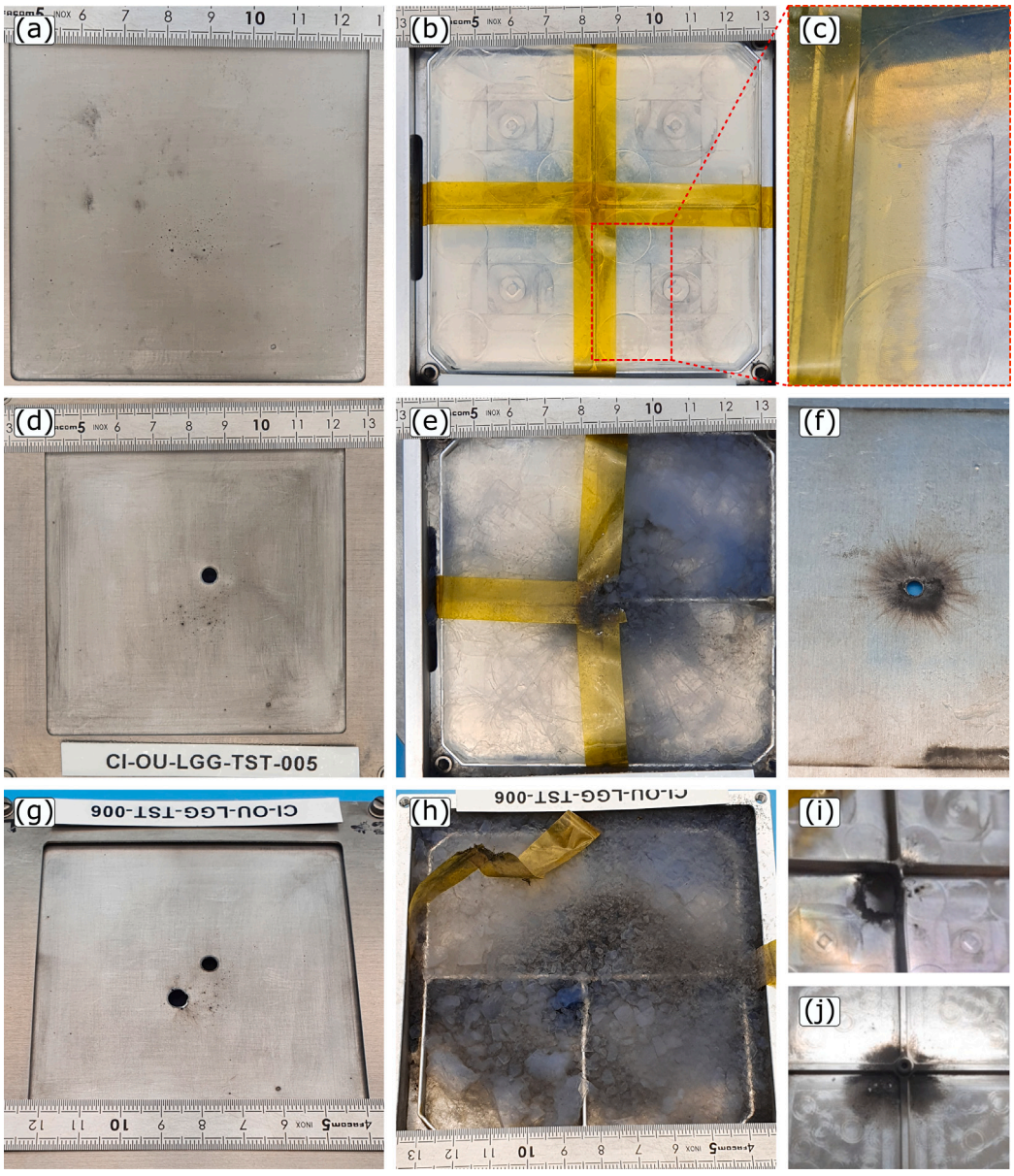

Fig. 6. DISC breadboard #2 after impact of (in order): a buckshot of (250–500) μm forsterite particles at ∼5 km/s (sensing plate (a), aerogel: global view (b), detailed view (c)); a 2 mm aluminum sphere at 5 km/s (sensing plate (d), aerogel blocks (e), back side of sensing plate (f)); a 3 mm aluminum sphere at 5.00 km/s (sensing plate (g), aerogel blocks (h), dust shield frame (i), bottom box structure of DISC envelope (j)).

Table 6
Equivalent diameter d_K^* for which a spherical cometary dust particle of 570 kg/m^3 density at 70 km/s would have the same kinetic energy of the reported LGG shots. The probabilities of a collision on DISC units onboard S/Cs A (P_K^{A}) and B2 (P_K^{B2}) are also reported. Shots #6, 8, 9 perforated DISC dust shield.

Shot #	d_K^* (mm) @70 km/s	P_K^{A}	P_K^{B2}
1	0.38	0.236	0.923
5 , 7	0.58	0.089	0.590
3	0.69	0.058	0.436
9	0.82	0.037	0.304
6 , 8	0.87	0.032	0.270

general method that takes into account the physical and geometrical features of both the projectile and the target. Ryan et al. (2010) studied the performance of open cell metallic foam core sandwich panel structures for micrometeoroid and orbital debris shielding [58]. They derived three ballistic limit equations (BLEs) for three different regimes of the projectile speed. Since the open cell metallic foam core structure is similar to the DISC dust shield, we considered the BLE for hypervelocity projectiles ($v_i > 4$ km/s) fired along the symmetry axis of the target. In [58], the particles turned into a finely dispersed predominantly molten debris cloud on impact, similarly to some of our results (see Fig. 5, panel (h), and Fig. 6, panel (f)). In order to verify whether the physical processes described by Ryan et al. (2010) describes our situation, we substituted the metallic foam features with the aerogel ones and computed the critical diameter d_c for the projectiles in the frame of our tests with the LGG as

$$d_c = 1.915\,\frac{\left(t_r + 0.5\,AD_{aer}/\rho_r\right)^{2/3}\; t_{aer}^{0.45}\; \left(\sigma_r/70\right)^{1/3}}{\rho_i^{1/3}\;\rho_f^{1/9}\;v_i^{2/5}}\,. \tag{3}$$

The critical diameter d_c is the largest size for which a (spherical) projectile of density ρ_i and impact speed v_i does not perforate a structure designed as DISC dust shield, where ρ_f is the density of the front sheet (the DISC sensing plate), AD_{aer} and t_{aer} are the aerogel surface density and thickness, ρ_r, t_r, and σ_r are the dust shield frame density, thickness and yield strength. The results obtained with the BLE (3) were then

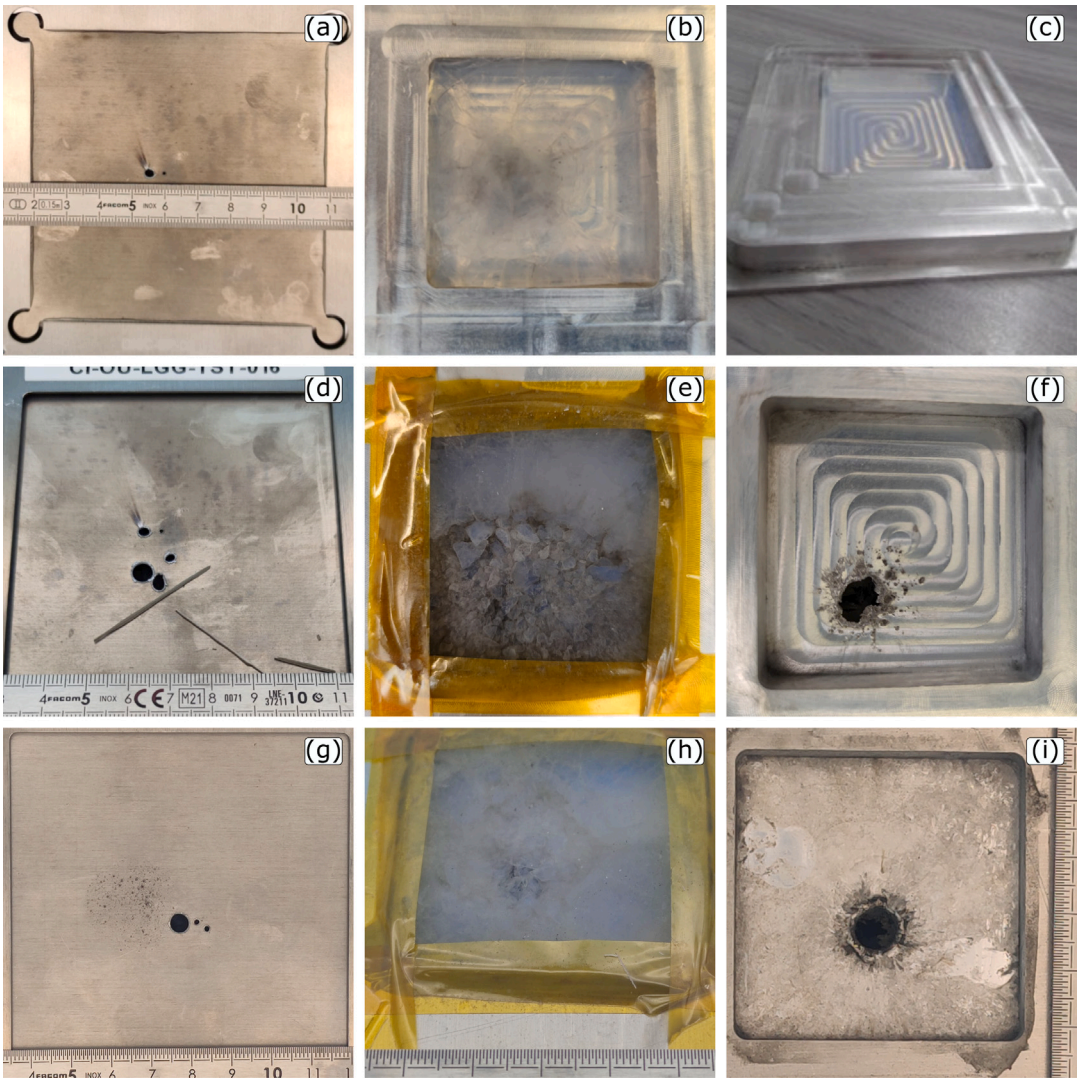

Fig. 7. DISC breadboards #3 and #4 after the collision with (in order): a 2 mm aluminum sphere at 5 km/s (breadboard #3: sensing plate (a), aerogel (b)); a 3 mm aluminum sphere at 5 km/s (breadboard #3: sensing plate (d), aerogel (e), dust shield frame (f)); a 3 mm borosilicate glass sphere at 4.4 km/s (breadboard #4: sensing plate (g), aerogel (h), dust shield frame (i)). Panel (c) shows the new dust shield frame design integrated in these two breadboards.

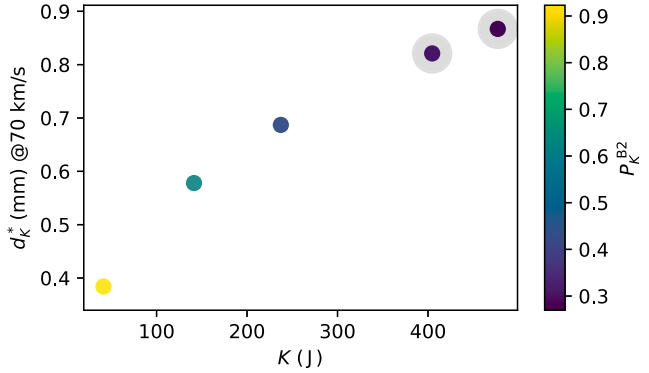

Fig. 8. Equivalent diameter d_K^* for which a (spherical) cometary dust particle with density of 570 kg/m^3 at 70 km/s would have the kinetic energy K of the corresponding LGG test, reported on the horizontal axis. The color encodes the probability P_K^{B2} that a particle collides on the DISC unit onboard S/C B2. The greyish circles identify the kinetic energy values resulted in a DISC failure.

compared to the real diameter of the projectiles shot with the LGG. Fig. 9 shows the real diameter d of the LGG projectiles normalized to the corresponding critical diameter value d_c obtained with the BLE (3). By comparing the results of the LGG tests performed with the current dust shield design (full dots) and the theoretical predictions of the instrument upper resistance limit by the BLE (red dashed line), we deduce that Eq. (3) underestimates DISC dust shield real performance. Successful shots #3,5,7 stand above the BLE reference (i.e. $d > d_c$), meaning that the DISC dust shield protects the instrument from projectiles that were theoretically expected to procure a failure in the unit. In particular, shot #3 defines the empirical new upper resistance limit of the instrument, highlighted with the green dashed line.

We tentatively extrapolate the BLE (3) to obtain the critical diameter d_c^* of a cometary dust particle with a density of 570 kg/m3 impacting at 70 km/s, retrieving, for the dust shield used for the laboratory tests $d_c^* = 0.98$ mm, which corresponds to a dust particle with 20% probability to collide on S/C B2, too high with respect to the S/C safety requirements. Under the assumption that equal impact energies at low and high impact velocities produce comparable damages, we extrapolated the BLE considering a thicker aerogel layer ($t_{aer} = 20$ mm), resulting in a critical diameter $d_c^* = 1.34$ mm, i.e. a cometary particle with an impact probability on S/C B2 of 9.6%, compliant with the safety requirements (<10%).

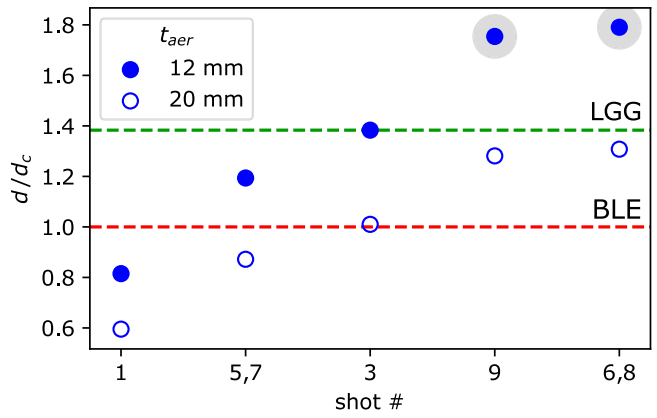

Fig. 9. Diameter d of the particles shot for our tests with the LGG, normalized to the corresponding critical diameter d_c obtained with Eq. (3). Full circles show the results obtained with the current dust shield design; empty circles represent the values scaled to an upgraded design with an aerogel thickness of t_{aer} = 20 mm. The dust shield failures are highlighted in gray; the two dashed lines show the upper resistance limit according to the ballistic limit equation (red) and to our tests with the LGG (green).

4. Conclusion

We designed and manufactured an innovative light and compact dust shield that will mitigate the dust hazard for DISC, an instrument that will characterize μm-to-mm sized dust particles in the coma of a dynamically new comet, onboard Comet Interceptor/ESA S/C A and S/C B2. In this work we assessed the DISC dust shield response to hypervelocity impacts with the aim of defining its performance during the flyby, focusing on the most critical conditions (closest approach distance of ∼200 km and maximum flyby speed of ∼70 km/s). We performed hypervelocity impact tests, compensating the high speed values not reachable in the laboratory with projectiles having masses higher than those expected along the flyby, resulting in impacts with equivalent kinetic energies. Using a Light-Gas Gun, we shot mm-sized particles of various materials at speeds up to 6 km/s, i.e. impacts with kinetic energies from 41 J to 477 J. The results we obtained assure the DISC dust shield reliability for impacts with kinetic energy up to about 240 J. The next step test was performed at an energy of ∼400 J for which the dust shield failed. A preliminary conclusion for the dust shield design that implies a 12 mm-thick aerogel tile is that the maximum kinetic energy for which it is reliable is within the range 240–400 J. As a first tentative step to define more accurately the kinetic energy upper limit for the dust shield failure we combined these laboratory results with theoretical predictions by a ballistic limit equation for hypervelocity impacts on a similar dust shield configuration. This equation allowed us to determine the size (critical diameter d_c^* = 0.98 mm) of a cometary dust particle (density of 570 kg/m^3) impacting the DISC dust shield at 70 km/s and causing its failure while assuming that equal impact energies at low and high impact velocities produce comparable damages. Combined with the Engineering Dust Coma Model simulations, we concluded that the dust shield design with a 12 mm-thick aerogel block would have a not acceptable probability of failure in protecting DISC onboard S/C B2, flying at 70 km/s with a flyby closest approach distance from the nucleus of 200 km. To overcome this risk of failure, we performed new calculation for an upgraded design of the DISC dust shield, implying an increased aerogel layer thickness of 20 mm (without any modifications to the mechanics). We determine the updated maximum dust particle size inducing the dust shield failure (i.e. the critical diameter) as d_c^* = 1.34 mm, having an impact probability on the S/C B2 flying at 70 km/s of 9.6%, which is compatible with the threshold value for the S/C safety (10%). We conclude that the DISC dust shield upgraded design (20 mm-thick aerogel) guarantees DISC safety and measurement compatibility within the expected cometary dust environment that Comet Interceptor will encounter.

CRediT authorship contribution statement

Vincenzo Della Corte: Writing – review & editing, Supervision, Methodology, Investigation, Funding acquisition, Conceptualization. **Stefano Ferretti:** Writing – original draft, Conceptualization. **Alice Maria Piccirillo:** Writing – review & editing, Investigation, Conceptualization. **Alessandra Rotundi:** Writing – review & editing, Supervision, Funding acquisition, Conceptualization. **Ivano Bertini:** Writing – review & editing, Investigation. **Fabio Cozzolino:** Writing – review & editing. **Alessio Ferone:** Writing – review & editing. **Stefano Fiscale:** Writing – review & editing. **Andrea Longobardo:** Writing – review & editing. **Laura Inno:** Writing – review & editing. **Eleonora Ammannito:** Writing – review & editing, Resources. **Giuseppe Sindoni:** Writing – review & editing, Resources. **Chiara Grappasonni:** Writing – review & editing, Resources. **Matthew Sylvest:** Data curation. **Manish R. Patel:** Investigation, Data curation. **Hanno Ertel:** Validation, Investigation. **Mark Millinger:** Supervision. **Hanna Rothkaehl:** Investigation.

Declaration of competing interest

The authors declare the following financial interests/personal relationships which may be considered as potential competing interests: Vincenzo Della Corte reports financial support was provided by European Space Agency. Vincenzo Della Corte reports financial support was provided by Italian Space Agency. If there are other authors, they declare that they have no known competing financial interests or personal relationships that could have appeared to influence the work reported in this paper.

Acknowledgments

We thank: the Italian Space Agency (ASI) within the ASI-INAF agreements I/024/12/0, 2020-4-HH.0 and 2023-14-HH.0; ESA that supported this study with the contract 3-17164/21/NL/GP/pbe COMET INTERCEPTOR-IT-3; the PhD program PON “Ricerca e Innovazione” 2014–2020, DM n. 1233 (30/07/2020).

Data availability

Data will be made available on request.

References

[1] Baker GL. Emanuel Swedenborg-an 18th century cosmologist. Phys Teach 1983;21(7):441–6.
[2] Woolfson MM. The solar system – its origin and evolution. Q J R Astron Soc 1993;34:1–20.
[3] Blum J, Gundlach B, Krause M, Fulle M, Johansen A, Agarwal J, Von Borstel I, Shi X, Hu X, Bentley MS, et al. Evidence for the formation of comet 67p/Churyumov–Gerasimenko through gravitational collapse of a bound clump of pebbles. Mon Not R Astron Soc 2017;469(Suppl_2):S755–73.
[4] Keller HU, Kührt E. Cometary nuclei—From Giotto to Rosetta. Space Sci Rev 2020;216(1):1–26.
[5] Reinhard R. The Giotto encounter with comet Halley. Nature 1986;321(6067):313–8.
[6] Taylor M, Altobelli N, Buratti B, Choukroun M. The Rosetta mission orbiter science overview: the comet phase. Phil Trans R Soc A 2017;375(2097):20160262.
[7] Sagdeev RZ, Blamont J, Galeev A, Moroz V, Shapiro V, Shevchenko V, Szegő K. Vega spacecraft encounters with comet Halley. Nature 1986;321(6067):259–62.
[8] Keller HU, Arpigny C, Barbieri C, Bonnet R, Cazes S, Coradini M, Cosmovici C, Delamere W, Huebner W, Hughes D, et al. First Halley multicolour camera imaging results from Giotto. Nature 1986;321(6067):320–6.
[9] Kissel J, Sagdeev R, Bertaux J-L, Angarov V, Audouze J, Blamont J-E, Büchler K, Evlanov E, Fechtig H, Fomenkova M, et al. Composition of comet Halley dust particles from Vega observations. Nature 1986;321(6067):280–2.
[10] Altwegg K, Balsiger H, Bar-Nun A, Berthelier J-J, Bieler A, Bochsler P, Briois C, Calmonte U, Combi M, De Keyser J, et al. 67P/Churyumov–Gerasimenko, a jupiter family comet with a high D/H ratio. Science 2015;347(6220):1261952.

[11] Sierks H, Barbieri C, Lamy PL, Rodrigo R, Koschny D, Rickman H, Keller HU, Agarwal J, A'hearn MF, Angrilli F, et al. On the nucleus structure and activity of comet 67p/Churyumov–Gerasimenko. Science 2015;347(6220):aaa1044.
[12] Hässig M, Altwegg K, Balsiger H, Bar-Nun A, Berthelier J-J, Bieler A, Bochsler P, Briois C, Calmonte U, Combi M, et al. Time variability and heterogeneity in the coma of 67p/Churyumov–Gerasimenko. Science 2015;347(6220):aaa0276.
[13] El-Maarry MR, Thomas N, Giacomini L, Massironi M, Pajola M, Marschall R, Gracia-Berná A, Sierks H, Barbieri C, Lamy PL, et al. Regional surface morphology of comet 67p/Churyumov–Gerasimenko from Rosetta/OSIRIS images. Astron Astrophys 2015;583:A26.
[14] El-Maarry MR, Thomas N, Gracia-Berná A, Pajola M, Lee J-C, Massironi M, Davidsson B, Marchi S, Keller H, Hviid S, et al. Regional surface morphology of comet 67p/Churyumov–Gerasimenko from Rosetta/OSIRIS images: The southern hemisphere. Astron Astrophys 2016;593:A110.
[15] Della Corte V, Rotundi A, Fulle M, Gruen E, Weissman P, Sordini R, Ferrari M, Ivanovski S, Lucarelli F, Accolla M, et al. GIADA: shining a light on the monitoring of the comet dust production from the nucleus of 67p/Churyumov–Gerasimenko. Astron Astrophys 2015;583:A13.
[16] Rotundi A, Sierks H, Della Corte V, Fulle M, Gutierrez PJ, Lara L, Barbieri C, Lamy PL, Rodrigo R, Koschny D, et al. Dust measurements in the coma of comet 67p/Churyumov–Gerasimenko inbound to the sun. Science 2015;347(6220):aaa3905.
[17] Della Corte V, Rotundi A, Fulle M, Ivanovski S, Green SF, Rietmeijer FJ, Colangeli L, Palumbo P, Sordini R, Ferrari M, et al. 67P/CG inner coma dust properties from 2.2 au inbound to 2.0 au outbound to the sun. Mon Not R Astron Soc 2016;462(Suppl_1):S210–9.
[18] Della Corte V, Rotundi A, Zakharov V, Ivanovski S, Palumbo P, Fulle M, Longobardo A, Dionnet Z, Liuzzi V, Salatti M. GIADA microbalance measurements on board Rosetta: submicrometer-to micrometer-sized dust particle flux in the coma of comet 67p/Churyumov–Gerasimenko. Astron Astrophys 2019;630:A25.
[19] Fulle M, Della Corte V, Rotundi A, Green S, Accolla M, Colangeli L, Ferrari M, Ivanovski S, Sordini R, Zakharov V. The dust-to-ices ratio in comets and Kuiper belt objects. Mon Not R Astron Soc 2017;469(Suppl_2):S45–9.
[20] Fulle M, Blum J, Rotundi A, Gundlach B, Güttler C, Zakharov V. How comets work: nucleus erosion versus dehydration. Mon Not R Astron Soc 2020;493(3):4039–44.
[21] Oort JH. The structure of the cloud of comets surrounding the solar system and a hypothesis concerning its origin. Bull Astron Inst Netherlands 1950;11:91–110.
[22] Snodgrass C, Jones GH. The European space agency's comet interceptor lies in wait. Nature Commun 2019;10(1):1–4.
[23] Esposito F, Colangeli L, Della Corte V, Palumbo P. Physical aspect of an "impact sensor" for the detection of cometary dust momentum onboard the "Rosetta" space mission. Adv Space Res 2002;29(8):1159–63.
[24] Della Corte V, Sordini R, Accolla M, Ferrari M, Ivanovski S, Rotundi A, Rietmeijer F, Fulle M, Mazzotta-Epifani E, Palumbo P, et al. Giada–grain impact analyzer and dust accumulator–onboard Rosetta spacecraft: extended calibrations. Acta Astronaut 2016;126:205–14.
[25] Rothkaehl H, Andre N, Auster U, Della Corte V, Edberg N, Galand M, Henri P, de Keyser J, Kolmasova I, Morawski M, et al. Dust, field and plasma instrument onboard ESA's comet interceptor mission. In: Europlanet science congress 2021. 2021.
[26] Della Corte V, Rotundi A, Bertini I, Di Paolo F, Inno L, Longobardo A, Piccirillo A, Zakharov V, Ferraioli G, Ammannito E, et al. DISC, the dust impact sensor and counter, on board comet interceptor ESA space mission, for in situ dust environment characterization of a dynamically new comet. In: 52nd lunar and planetary science conference. no. 2548, 2021, p. 2332.
[27] Della Corte V, Ferretti S, Piccirillo A, Zakharov V, Di Paolo F, Rotundi A, Ammannito E, Amoroso M, Bertini I, Di Donato P, et al. DISC-the dust impact sensor and counter on-board comet interceptor: characterization of the dust coma of a dynamically new comet. Adv Space Res 2023.
[28] Whipple FL. Meteorites and space travel. Astron J 1947;52:131.
[29] Osegueda RA, Carrasco CJ, Orozco M, Eftis J, Reynolds E, Sholar TG. Contour dust shield performance. J Aerosp Eng 2001;14(4):147–57.
[30] Brownlee D, Tsou P, Anderson J, Hanner M, Newburn R, Sekanina Z, Clark B, Hörz F, Zolensky M, Kissel J, et al. Stardust: Comet and interstellar dust sample return mission. J Geophys Res Planets 2003;108(E10).
[31] Divine N, Fechtig H, Gombosi T, Hanner M, Keller H, Larson S, Mendis D, Newburn RL, Reinhard R, Sekanina Z, et al. The comet Halley dust and gas environment. Space Sci Rev 1986;43(1):1–104.
[32] Lamb H. On the vibrations of an elastic sphere. Proc Lond Math Soc 1881;1(1):189–212.
[33] Liu M, Su Z, Zhang Q, Long R. Modeling hypervelocity-impact-induced shock waves for characterizing orbital debris-produced damage. J Appl Mech 2016;83(8).
[34] Di Paolo F, Della Corte V, Bertini I, Inno L, Longobardo A, Piccirillo A, Rotundi A. Dust impact sensor and counter (DISC) for comet exploration: Laser simulations of hypervelocity impacts. In: 52nd lunar and planetary science conference. no. 2548, 2021, p. 1238.
[35] Zakharov V, Rotundi A, Della Corte V, Fulle M, Ivanovski S, Rodionov A, Bykov N. On the similarity of dust flows in the inner coma of comets. Icarus 2021;364:114476.
[36] McDonnell J. The open university planetary impact facility: A compact two-stage light gas gun for all impact angles. Int J Impact Eng 2006;33(1–12):410–8.
[37] Hibbert R, Cole M, Price MC, Burchell M. The hypervelocity impact facility at the university of kent: Recent upgrades and specialized capabilities. Procedia Eng 2017;204:208–14.
[38] Maag C. Results of space shuttle intact particle capture experiments. Hypervelocity Impacts Space 1992;186–90.
[39] Tsou P. Silica aerogel captures cosmic dust intact. J Non-Cryst Solids 1995;186:415–27.
[40] Brownlee D, Horz F, Hrubsch L, McDonnell J, Tsou P, Williams J. Eureka!! Aerogel capture of meteoroids in space. In: Lunar and planetary science conference. Vol. 25, 1994.
[41] Burchell MJ, Cole MJ, McDonnell J, Zarnecki JC. Hypervelocity impact studies using the 2 MV Van de Graaff accelerator and two-stage light gas gun of the University of Kent at Canterbury. Meas Sci Technol 1999;10(1):41.
[42] Shrine NR, McDonnell J, Burchell MJ, Gardner DJ, Jolly HS, Ratcliff P, Thomson R. EuroMir'95: First results from the dustwatch-P detectors of the European space exposure facility. Adv Space Res 1997;20(8):1481–4.
[43] Horz F. ODC: Aerogel particle capture during 18 months exposure on Mir. In: Abst. lunar planet. sci. conf.. Vol. 29, 1998.
[44] Hörz F, Cress G, Zolensky M, See TH, Bernhard RP, Warren JL. Optical analysis of impact features in aerogel from the orbital debris collection experiment on the MIR station. Tech. rep., National Aeronautics and Space Administration, Lyndon B. Johnson Space Center; 1999.
[45] Hörz F, Zolensky M, Bernhard R, See T, Warren J. Impact features and projectile residues in aerogel exposed on Mir. Icarus 2000;147(2):559–79.
[46] Rotundi A, Rietmeijer F, Ferrari M, Della Corte V, Baratta G, Brunetto R, Dartois E, Djouadi Z, Merouane S, Borg J, et al. Two refractory wild 2 terminal particles from a carrot-shaped track characterized combining MIR/FIR/Raman microspectroscopy and FE-SEM/EDS analyses. Meteorit Planet Sci 2014;49(4):550–75.
[47] Rotundi A, Baratta G, Borg J, Brucato J, Busemann H, Colangeli L, d'Hendecourt L, Djouadi Z, Ferrini G, Franchi I, et al. Combined micro-Raman, micro-infrared, and field emission scanning electron microscope analyses of comet 81p/wild 2 particles collected by stardust. Meteorit Planet Sci 2008;43(1–2):367–97.
[48] Brownlee D, Tsou P, Aléon J, Alexander CMO, Araki T, Bajt S, Baratta GA, Bastien R, Bland P, Bleuet P, et al. Comet 81p/wild 2 under a microscope. Science 2006;314(5806):1711–6.
[49] Burchell MJ, Creighton J, Cole MJ, Mann J, Kearsley AT. Capture of particles in hypervelocity impacts in aerogel. Meteorit Planet Sci 2001;36(2):209–21.
[50] Trucano TG, Grady DE. Impact shock and penetration fragmentation in porous media. Int J Impact Eng 1995;17(4–6):861–72.
[51] Kitazawa Y, Fujiwara A, Kadono T, Imagawa K, Okada Y, Uematsu K. Hypervelocity impact experiments on aerogel dust collector. J Geophys Res Planets 1999;104(E9):22035–52.
[52] Domínguez G, Westphal AJ, Jones SM, Phillips ML. Energy loss and impact cratering in aerogels: Theory and experiment. Icarus 2004;172(2):613–24.
[53] Marschall R, Zakharov V, Tubiana C, Kelley MS, van Damme CC, Snodgrass C, Jones GH, Ivanovski SL, Postberg F, Della Corte V, et al. Determining the dust environment of an unknown comet for a spacecraft flyby: The case of ESA's Comet interceptor mission. Astron Astrophys 2022;666:A151.
[54] Piekutowski A, Poormon K. Effects of scale on the performance of whipple shields for impact velocities ranging from 7 to 10 km/s. Procedia Eng 2013;58:642–52. http://dx.doi.org/10.1016/j.proeng.2013.05.074, URL https://www.sciencedirect.com/science/article/pii/S1877705813009806. Proceedings of the 12th Hypervelocity Impact Symposium.
[55] Piekutowski AJ. Holes produced in thin aluminum sheets by the hypervelocity impact of aluminum spheres. Int J Impact Eng 1999;23(1, Part 2):711–22. http://dx.doi.org/10.1016/S0734-743X(99)00116-5, URL https://www.sciencedirect.com/science/article/pii/S0734743X99001165.
[56] Hertzberg A. On the possibility of simulating meteoroid impact by the use of lasers topical report. 1964.
[57] Dienes J, Walsh J. Theory of impact: Some general principles and the method of Eulerian codes. In: High-velocity impact phenomena. Vol. 2, Academic Press New York; 1970, p. 25–104.
[58] Ryan S, Ordonez E, Christiansen E, Lear D. Hypervelocity impact performance of open cell foam core sandwich panel structures. In: Hypervelocity impact symposium. no. JSC-CN-19432, 2010.